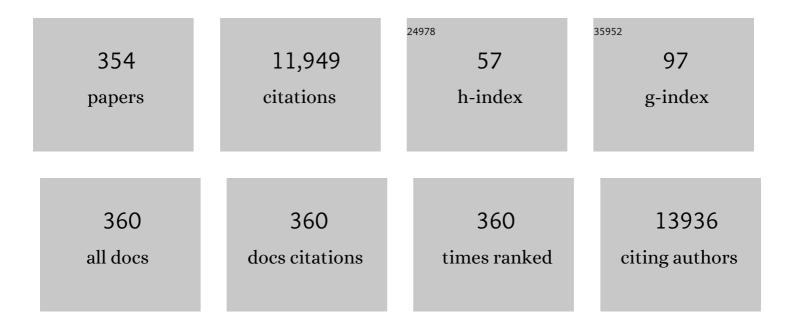
List of Publications by Year in descending order

Source: https://exaly.com/author-pdf/5310731/publications.pdf Version: 2024-02-01



OLE HANSEN

#	Article	IF	CITATIONS
1	Bioinspired molecular co-catalysts bonded to a silicon photocathode for solar hydrogen evolution. Nature Materials, 2011, 10, 434-438.	13.3	600
2	Strained silicon as a new electro-optic material. Nature, 2006, 441, 199-202.	13.7	599
3	Strategies for stable water splitting via protected photoelectrodes. Chemical Society Reviews, 2017, 46, 1933-1954.	18.7	427
4	Using TiO <sub>2</sub> as a Conductive Protective Layer for Photocathodic H <sub>2</sub> Evolution. Journal of the American Chemical Society, 2013, 135, 1057-1064.	6.6	426
5	Impact of nanoparticle size and lattice oxygen on water oxidation on NiFeOxHy. Nature Catalysis, 2018, 1, 820-829.	16.1	344
6	Hydrogen Production Using a Molybdenum Sulfide Catalyst on a Titaniumâ€Protected n <sup>+</sup> p‧ilicon Photocathode. Angewandte Chemie - International Edition, 2012, 51, 9128-9131.	7.2	289
7	Environmental sensors based on micromachined cantilevers with integrated read-out. Ultramicroscopy, 2000, 82, 11-16.	0.8	266
8	Enhanced Light–Matter Interactions in Graphene-Covered Gold Nanovoid Arrays. Nano Letters, 2013, 13, 4690-4696.	4.5	204
9	Mass and position determination of attached particles on cantilever based mass sensors. Review of Scientific Instruments, 2007, 78, 103303.	0.6	179
10	Undoped and <i>in-situ</i> B doped GeSn epitaxial growth on Ge by atmospheric pressure-chemical vapor deposition. Applied Physics Letters, 2011, 99, .	1.5	168
11	Optimised cantilever biosensor with piezoresistive read-out. Ultramicroscopy, 2003, 97, 371-376.	0.8	167
12	Scalability and feasibility of photoelectrochemical H <sub>2</sub> evolution: the ultimate limit of Pt nanoparticle as an HER catalyst. Energy and Environmental Science, 2015, 8, 2991-2999.	15.6	162
13	Graphene Conductance Uniformity Mapping. Nano Letters, 2012, 12, 5074-5081.	4.5	152
14	Atomic force microscopy probe with piezoresistive read-out and a highly symmetrical Wheatstone bridge arrangement. Sensors and Actuators A: Physical, 2000, 83, 47-53.	2.0	146
15	Optimization of sensitivity and noise in piezoresistive cantilevers. Journal of Applied Physics, 2002, 92, 6296-6301.	1.1	141
16	A microcantilever-based alcohol vapor sensor-application and response model. Applied Physics Letters, 2000, 76, 2615-2617.	1.5	140
17	Magnetic separation in microfluidic systems using microfabricated electromagnets—experiments and simulations. Journal of Magnetism and Magnetic Materials, 2005, 293, 597-604.	1.0	133
18	2-Photon tandem device for water splitting: comparing photocathode first <i>versus</i> photoanode first designs. Energy and Environmental Science, 2014, 7, 2397-2413.	15.6	130

#	Article	IF	CITATIONS
19	Selective filling of photonic crystal fibers using focused ion beam milled microchannels. Optics Express, 2011, 19, 17585.	1.7	124
20	What is the band alignment of Cu 2 ZnSn(S,Se) 4 solar cells?. Solar Energy Materials and Solar Cells, 2017, 169, 177-194.	3.0	124
21	Electrostatic energy harvesting device with out-of-the-plane gap closing scheme. Sensors and Actuators A: Physical, 2014, 211, 131-137.	2.0	121
22	Fabrication and characterization of nanoresonating devices for mass detection. Journal of Vacuum Science & Technology an Official Journal of the American Vacuum Society B, Microelectronics Processing and Phenomena, 2000, 18, 612.	1.6	116
23	Experimental observation of plasmons in a graphene monolayer resting on a two-dimensional subwavelength silicon grating. Applied Physics Letters, 2013, 102, .	1.5	109
24	Silicon protected with atomic layer deposited TiO2: durability studies of photocathodic H2 evolution. RSC Advances, 2013, 3, 25902.	1.7	104
25	Bi-resonant structure with piezoelectric PVDF films for energy harvesting from random vibration sources at low frequency. Sensors and Actuators A: Physical, 2016, 247, 547-554.	2.0	104
26	Electro-thermally actuated microgrippers with integrated force-feedback. Journal of Micromechanics and Microengineering, 2005, 15, 1265-1270.	1.5	99
27	Protection of p <sup>+</sup> -n-Si Photoanodes by Sputter-Deposited Ir/IrO <sub><i>x</i></sub> Thin Films. Journal of Physical Chemistry Letters, 2014, 5, 1948-1952.	2.1	97
28	Catalytic ammonia decomposition: miniaturized production of CO -free hydrogen for fuel cells. Catalysis Communications, 2005, 6, 229-232.	1.6	94
29	Iron-Treated NiO as a Highly Transparent p-Type Protection Layer for Efficient Si-Based Photoanodes. Journal of Physical Chemistry Letters, 2014, 5, 3456-3461.	2.1	93
30	Modeling and Optimization of an Electrostatic Energy Harvesting Device. Journal of Microelectromechanical Systems, 2014, 23, 1141-1155.	1.7	92
31	Sulfide perovskites for solar energy conversion applications: computational screening and synthesis of the selected compound LaYS <sub>3</sub> . Energy and Environmental Science, 2017, 10, 2579-2593.	15.6	91
32	MoS2—an integrated protective and active layer on n+p-Si for solar H2 evolution. Physical Chemistry Chemical Physics, 2013, 15, 20000.	1.3	89
33	Scanning microscopic four-point conductivity probes. Sensors and Actuators A: Physical, 2002, 96, 53-58.	2.0	87
34	Atomic Layer Deposition of Ruthenium with TiN Interface for Sub-10 nm Advanced Interconnects beyond Copper. ACS Applied Materials & amp; Interfaces, 2016, 8, 26119-26125.	4.0	87
35	Surface-directed capillary system; theory, experiments and applications. Lab on A Chip, 2005, 5, 827.	3.1	85
36	Crystalline TiO <sub>2</sub> : A Generic and Effective Electron-Conducting Protection Layer for Photoanodes and -cathodes. Journal of Physical Chemistry C, 2015, 119, 15019-15027.	1.5	85

#	Article	IF	CITATIONS
37	Ultra-thin Cu2ZnSnS4 solar cell by pulsed laser deposition. Solar Energy Materials and Solar Cells, 2017, 166, 91-99.	3.0	83
38	AFM probes with directly fabricated tips. Journal of Micromechanics and Microengineering, 1996, 6, 58-62.	1.5	81
39	Thermal stability of vapor phase deposited self-assembled monolayers for MEMS anti-stiction. Journal of Micromechanics and Microengineering, 2006, 16, 2259-2264.	1.5	79
40	Vapor-Phase Self-Assembled Monolayers for Anti-Stiction Applications in MEMS. Journal of Microelectromechanical Systems, 2007, 16, 1451-1460.	1.7	77
41	Discrete Dynamics of Nanoparticle Channelling in Suspended Graphene. Nano Letters, 2011, 11, 2689-2692.	4.5	77
42	Screen printed PZT/PZT thick film bimorph MEMS cantilever device for vibration energy harvesting. Sensors and Actuators A: Physical, 2012, 188, 383-388.	2.0	77
43	Back-illuminated Si photocathode: a combined experimental and theoretical study for photocatalytic hydrogen evolution. Energy and Environmental Science, 2015, 8, 650-660.	15.6	76
44	Micro-four-point probe Hall effect measurement method. Journal of Applied Physics, 2008, 104, .	1.1	74
45	Electrically Continuous Graphene from Single Crystal Copper Verified by Terahertz Conductance Spectroscopy and Micro Four-Point Probe. Nano Letters, 2014, 14, 6348-6355.	4.5	74
46	Gas phase photocatalytic water splitting with Rh2â^'yCryO3/GaN:ZnO in μ-reactors. Energy and Environmental Science, 2011, 4, 2937.	15.6	71
47	An electret-based energy harvesting device with a wafer-level fabrication process. Journal of Micromechanics and Microengineering, 2013, 23, 114010.	1.5	70
48	AFM lithography of aluminum for fabrication of nanomechanical systems. Ultramicroscopy, 2003, 97, 467-472.	0.8	67
49	MEMS device for bending test: measurements of fatigue and creep of electroplated nickel. Sensors and Actuators A: Physical, 2003, 103, 156-164.	2.0	67
50	Electroplating and characterization of cobalt–nickel–iron and nickel–iron for magnetic microsystems applications. Sensors and Actuators A: Physical, 2001, 92, 242-248.	2.0	64
51	Flame spray deposition of porous catalysts on surfaces and in microsystems. Journal of Catalysis, 2004, 223, 271-277.	3.1	63
52	Dielectric function and double absorption onset of monoclinic Cu 2 SnS 3 : Origin of experimental features explained by first-principles calculations. Solar Energy Materials and Solar Cells, 2016, 154, 121-129.	3.0	62
53	Noise in piezoresistive atomic force microscopy. Nanotechnology, 1999, 10, 51-60.	1.3	61
54	Black silicon laser-doped selective emitter solar cell with 18.1% efficiency. Solar Energy Materials and Solar Cells, 2016, 144, 740-747.	3.0	61

#	Article	IF	CITATIONS
55	Comparison of the Performance of CoP-Coated and Pt-Coated Radial Junction n <sup>+</sup> p-Silicon Microwire-Array Photocathodes for the Sunlight-Driven Reduction of Water to H <sub>2</sub> (g). Journal of Physical Chemistry Letters, 2015, 6, 1679-1683.	2.1	60
56	Microelectromagnet for magnetic manipulation in lab-on-a-chip systems. Journal of Magnetism and Magnetic Materials, 2006, 300, 418-426.	1.0	59
57	Highly sensitive micromachined capacitive pressure sensor with reduced hysteresis and low parasitic capacitance. Sensors and Actuators A: Physical, 2009, 154, 35-41.	2.0	58
58	Promoted Ru on high-surface area graphite for efficient miniaturized production of hydrogen from ammonia. Catalysis Letters, 2006, 112, 77-81.	1.4	57
59	Accurate microfour-point probe sheet resistance measurements on small samples. Review of Scientific Instruments, 2009, 80, 053902.	0.6	55
60	Piezoresistance of silicon and strained Si0.9Ge0.1. Sensors and Actuators A: Physical, 2005, 123-124, 388-396.	2.0	53
61	Enabling real-time detection of electrochemical desorption phenomena with sub-monolayer sensitivity. Electrochimica Acta, 2018, 268, 520-530.	2.6	53
62	Piezoresistance in p-type silicon revisited. Journal of Applied Physics, 2008, 104, .	1.1	52
63	Protection of Si photocathode using TiO2 deposited by high power impulse magnetron sputtering for H2 evolution in alkaline media. Solar Energy Materials and Solar Cells, 2016, 144, 758-765.	3.0	52
64	Silicon protected with atomic layer deposited TiO2: conducting versus tunnelling through TiO2. Journal of Materials Chemistry A, 2013, 1, 15089.	5.2	51
65	Autonomous multi-sensor micro-system for measurement of ocean water salinity. Sensors and Actuators A: Physical, 2008, 147, 474-484.	2.0	48
66	Parallel Evaluation of the Bil <sub>3</sub> , BiOI, and Ag <sub>3</sub> Bil <sub>6</sub> Layered Photoabsorbers. Chemistry of Materials, 2020, 32, 3385-3395.	3.2	48
67	Investigations of the isotropic etch of an ICP source for silicon microlens mold fabrication. Journal of Micromechanics and Microengineering, 2005, 15, 873-882.	1.5	47
68	Highly sensitive silicon microreactor for catalyst testing. Review of Scientific Instruments, 2009, 80, 124101.	0.6	45
69	Suppression of the water splitting back reaction on GaN:ZnO photocatalysts loaded with core/shell cocatalysts, investigated using a 1¼-reactor. Journal of Catalysis, 2012, 292, 26-31.	3.1	45
70	Monolithic integration of mass sensing nano-cantilevers with CMOS circuitry. Sensors and Actuators A: Physical, 2003, 105, 311-319.	2.0	43
71	Analysis of small deflection touch mode behavior in capacitive pressure sensors. Sensors and Actuators A: Physical, 2010, 161, 114-119.	2.0	41
72	Photocatalytic methane decomposition over vertically aligned transparent TiO2 nanotube arrays. Chemical Communications, 2011, 47, 2613.	2.2	41

#	Article	IF	CITATIONS
73	Deposition of methylammonium iodide <i>via</i> evaporation – combined kinetic and mass spectrometric study. RSC Advances, 2018, 8, 29899-29908.	1.7	41
74	Review of electrical characterization of ultra-shallow junctions with micro four-point probes. Journal of Vacuum Science and Technology B:Nanotechnology and Microelectronics, 2010, 28, C1C27-C1C33.	0.6	40
75	Fabrication and characterization of MEMS-based PZT/PZT bimorph thick film vibration energy harvesters. Journal of Micromechanics and Microengineering, 2012, 22, 094007.	1.5	38
76	Energy band alignment at the heterointerface between CdS and Ag-alloyed CZTS. Scientific Reports, 2020, 10, 18388.	1.6	37
77	Invisible Surface Charge Pattern on Inorganic Electrets. IEEE Electron Device Letters, 2013, 34, 1047-1049.	2.2	35
78	Interface band gap narrowing behind open circuit voltage losses in Cu2ZnSnS4 solar cells. Applied Physics Letters, 2017, 110, .	1.5	35
79	How the relative permittivity of solar cell materials influences solar cell performance. Solar Energy, 2017, 149, 145-150.	2.9	35
80	Temperature dependent photoreflectance study of Cu2SnS3 thin films produced by pulsed laser deposition. Applied Physics Letters, 2017, 110, .	1.5	35
81	Carrier-selective p- and n-contacts for efficient and stable photocatalytic water reduction. Catalysis Today, 2017, 290, 59-64.	2.2	35
82	Persistent Double-Layer Formation in Kesterite Solar Cells: A Critical Review. ACS Applied Materials & Interfaces, 2020, 12, 39405-39424.	4.0	35
83	Cantilever surface stress sensors with single-crystalline silicon piezoresistors. Applied Physics Letters, 2005, 86, 203502.	1.5	34
84	Gas-phase photocatalysis in μ-reactors. Chemical Engineering Journal, 2010, 160, 738-741.	6.6	34
85	In Situ TEM Creation and Electrical Characterization of Nanowire Devices. Nano Letters, 2012, 12, 2965-2970.	4.5	34
86	Monolithic thin-film chalcogenide–silicon tandem solar cells enabled by a diffusion barrier. Solar Energy Materials and Solar Cells, 2020, 207, 110334.	3.0	34
87	Electron inelastic mean free path in water. Nanoscale, 2020, 12, 20649-20657.	2.8	34
88	Fabrication of submicron suspended structures by laser and atomic force microscopy lithography on aluminum combined with reactive ion etching. Journal of Vacuum Science & Technology an Official Journal of the American Vacuum Society B, Microelectronics Processing and Phenomena, 1998, 16, 2977.	1.6	33
89	Piezoresistive effect in top-down fabricated silicon nanowires. Proceedings of the IEEE International Conference on Micro Electro Mechanical Systems (MEMS), 2008, , .	0.0	33
90	Reactive ion etching of polymer materials for an energy harvesting device. Microelectronic Engineering, 2012, 97, 227-230.	1.1	33

#	Article	IF	CITATIONS
91	Photothermal Infrared Spectroscopy of Airborne Samples with Mechanical String Resonators. Analytical Chemistry, 2013, 85, 10531-10535.	3.2	33
92	Ultra Shallow Arsenic Junctions in Germanium Formed by Millisecond Laser Annealing. Electrochemical and Solid-State Letters, 2011, 14, H39.	2.2	32
93	A stretch-tunable plasmonic structure with a polarization-dependent response. Optics Express, 2012, 20, 5237.	1.7	32
94	Lattice-matched Cu2ZnSnS4/CeO2 solar cell with open circuit voltage boost. Applied Physics Letters, 2016, 109, .	1.5	32
95	Shining Light on Sulfide Perovskites: LaYS <sub>3</sub> Material Properties and Solar Cells. Chemistry of Materials, 2019, 31, 3359-3369.	3.2	32
96	Field-Induced Deformation as a Mechanism for Scanning Tunneling Microscopy Based Nanofabrication. Physical Review Letters, 1998, 81, 5572-5575.	2.9	31
97	Microfabricated high-temperature reactor for catalytic partial oxidation of methane. Applied Catalysis A: General, 2005, 284, 5-10.	2.2	31
98	SU-8 etching in inductively coupled oxygen plasma. Microelectronic Engineering, 2013, 112, 35-40.	1.1	31
99	Cantilever based mass sensor with hard contact readout. Applied Physics Letters, 2006, 88, 264104.	1.5	30
100	Dielectrophoresis microsystem with integrated flow cytometers for on-line monitoring of sorting efficiency. Electrophoresis, 2006, 27, 5081-5092.	1.3	29
101	Resolution enhancement of scanning four-point-probe measurements on two-dimensional systems. Review of Scientific Instruments, 2003, 74, 3701-3708.	0.6	27
102	Micro-four-point-probe characterization of nanowires fabricated using the nanostencil technique. Nanotechnology, 2004, 15, 1363-1367.	1.3	27
103	Four point bending setup for characterization of semiconductor piezoresistance. Review of Scientific Instruments, 2008, 79, 044703.	0.6	27
104	Quantitative Measurements of Photocatalytic CO-Oxidation as a Function of Light Intensity and Wavelength over TiO2 Nanotube Thin Films in μ-Reactors. Journal of Physical Chemistry C, 2010, 114, 11162-11168.	1.5	27
105	Low surface damage dry etched black silicon. Journal of Applied Physics, 2017, 122, .	1.1	27
106	Large process-dependent variations in band alignment and interface band gaps of Cu2ZnSnS4/CdS solar cells. Solar Energy Materials and Solar Cells, 2018, 187, 233-240.	3.0	27
107	Design of a silicon microphone with differential read-out of a sealed double parallel-plate capacitor. Sensors and Actuators A: Physical, 1996, 53, 232-236.	2.0	25
108	Static contact micro four-point probes with <11nm positioning repeatability. Microelectronic Engineering, 2008, 85, 1092-1095.	1.1	25

#	Article	IF	CITATIONS
109	On the analysis of the activation mechanisms of sub-melt laser anneals. Materials Science and Engineering B: Solid-State Materials for Advanced Technology, 2008, 154-155, 24-30.	1.7	25
110	Silicon as an anisotropic mechanical material: Deflection of thin crystalline plates. Sensors and Actuators A: Physical, 2014, 220, 347-364.	2.0	25
111	Mechanical Properties of Organic Nanofibers. Small, 2006, 2, 660-666.	5.2	24
112	Mo <sub>3</sub> S <sub>4</sub> Clusters as an Effective H <sub>2</sub> Evolution Catalyst on Protected Si Photocathodes. Journal of the Electrochemical Society, 2014, 161, H722-H724.	1.3	24
113	Durability Testing of Photoelectrochemical Hydrogen Production under Day/Night Light Cycled Conditions. ChemElectroChem, 2019, 6, 106-109.	1.7	24
114	Cell volume increase in murine MC3T3-E1 pre-osteoblasts attaching onto biocompatible Tantalum observed by magnetic AC mode Atomic Force Microscopy. , 2005, 10, 61-69.		24
115	Microcantilever equipped with nanowire template electrodes for multiprobe measurement on fragile nanostructures. Journal of Applied Physics, 2004, 96, 2895-2900.	1.1	23
116	Characterization of the microloading effect in deep reactive ion etching of silicon. , 2004, , .		23
117	Study of the Roughness in a Photoresist Masked, Isotropic, SF[sub 6]-Based ICP Silicon Etch. Journal of the Electrochemical Society, 2006, 153, G1051.	1.3	23
118	Fast thermal nanoimprint lithography by a stamp with integrated heater. Microelectronic Engineering, 2008, 85, 1229-1232.	1.1	23
119	Analytical Model of a PZT Thick-Film Triaxial Accelerometer for Optimum Design. IEEE Sensors Journal, 2009, 9, 419-429.	2.4	23
120	A generic model for photocatalytic activity as a function of catalyst thickness. Journal of Catalysis, 2012, 289, 62-72.	3.1	23
121	Resonant MEMS Tunable VCSEL. IEEE Journal of Selected Topics in Quantum Electronics, 2013, 19, 1702306-1702306.	1.9	23
122	Wide Band Gap Cu <sub>2</sub> SrSnS <sub>4</sub> Solar Cells from Oxide Precursors. ACS Applied Energy Materials, 2019, 2, 7340-7344.	2.5	23
123	Low-temperature anodic bonding to silicon nitride. Sensors and Actuators A: Physical, 2000, 82, 249-253.	2.0	22
124	Photoelectrocatalysis and electrocatalysis on silicon electrodes decorated with cubane-like clusters. Journal of Photonics for Energy, 2012, 2, 026001.	0.8	22
125	Thermodynamics of photon-enhanced thermionic emission solar cells. Applied Physics Letters, 2014, 104, 023902.	1.5	22
126	Fast and sensitive method for detecting volatile species in liquids. Review of Scientific Instruments, 2015, 86, 075006.	0.6	22

#	Article	IF	CITATIONS
127	Backâ€lluminated Siâ€Based Photoanode with Nickel Cobalt Oxide Catalytic Protection Layer. ChemElectroChem, 2016, 3, 1546-1552.	1.7	22
128	Nanomechanical Infrared Spectroscopy with Vibrating Filters for Pharmaceutical Analysis. Angewandte Chemie - International Edition, 2017, 56, 3901-3905.	7.2	22
129	A Flexible Webâ€Based Approach to Modeling Tandem Photocatalytic Devices. Solar Rrl, 2017, 1, e201600013.	3.1	22
130	Combined laser and atomic force microscope lithography on aluminum: Mask fabrication for nanoelectromechanical systems. Applied Physics Letters, 1999, 74, 3206-3208.	1.5	21
131	A comparison of detailed level and superconfiguration models of neon. Journal of Quantitative Spectroscopy and Radiative Transfer, 2006, 99, 272-282.	1.1	21
132	Note: Anodic bonding with cooling of heat-sensitive areas. Review of Scientific Instruments, 2010, 81, 016111.	0.6	21
133	Field Effect in Graphene-Based van der Waals Heterostructures: Stacking Sequence Matters. Nano Letters, 2017, 17, 2660-2666.	4.5	21
134	Diffusion in a short base. Solid-State Electronics, 1994, 37, 1663-1669.	0.8	20
135	Micromachined AFM transducer with differential capacitive read-out. Journal of Micromechanics and Microengineering, 1995, 5, 161-165.	1.5	20
136	Micromachined double backplate differential capacitive microphone. Journal of Micromechanics and Microengineering, 1999, 9, 30-33.	1.5	20
137	Angle resolved characterization of nanostructured and conventionally textured silicon solar cells. Solar Energy Materials and Solar Cells, 2015, 140, 134-140.	3.0	20
138	On performance limitations and property correlations of Al-doped ZnO deposited by radio-frequency sputtering. Journal Physics D: Applied Physics, 2016, 49, 295101.	1.3	20
139	Generation of micro-droplet arrays by dip-coating of biphilic surfaces; the dependence of entrained droplet volume on withdrawal velocity. Scientific Reports, 2017, 7, 12794.	1.6	20
140	Semitransparent Selenium Solar Cells as a Top Cell for Tandem Photovoltaics. Solar Rrl, 2021, 5, 2100111.	3.1	20
141	New approaches to atomic force microscope lithography on silicon. Journal of Vacuum Science & Technology an Official Journal of the American Vacuum Society B, Microelectronics Processing and Phenomena, 1997, 15, 2912.	1.6	19
142	Optical properties and surface characterization of pulsed laser-deposited Cu 2 ZnSnS 4 by spectroscopic ellipsometry. Thin Solid Films, 2015, 582, 203-207.	0.8	19
143	Surface passivation and carrier selectivity of the thermal-atomic-layer-deposited TiO <sub>2</sub> on crystalline silicon. Japanese Journal of Applied Physics, 2017, 56, 08MA11.	0.8	19
144	Low temperature bonding of heterogeneous materials using Al2O3 as an intermediate layer. Journal of Vacuum Science and Technology B:Nanotechnology and Microelectronics, 2018, 36, 011202.	0.6	19

#	Article	IF	CITATIONS
145	Nitride-Based Interfacial Layers for Monolithic Tandem Integration of New Solar Energy Materials on Si: The Case of CZTS. ACS Applied Energy Materials, 2020, 3, 4600-4609.	2.5	19
146	Impedance Based Characterization of a High-Coupled Screen Printed PZT Thick Film Unimorph Energy Harvester. Journal of Microelectromechanical Systems, 2014, 23, 842-854.	1.7	18
147	Balanced membrane micromachined loudspeaker for hearing instrument application. Journal of Micromechanics and Microengineering, 2001, 11, 334-338.	1.5	17
148	Microsystem with integrated capillary leak to mass spectrometer for high sensitivity temperature programmed desorption. Review of Scientific Instruments, 2004, 75, 3345-3347.	0.6	17
149	Sensitivity study of micro four-point probe measurements on small samples. Journal of Vacuum Science and Technology B:Nanotechnology and Microelectronics, 2010, 28, C1C34-C1C40.	0.6	17
150	Tracking neuronal marker expression inside living differentiating cells using molecular beacons. Frontiers in Cellular Neuroscience, 2013, 7, 266.	1.8	17
151	Synthesis of ligand-free CZTS nanoparticles via a facile hot injection route. Nanotechnology, 2016, 27, 185603.	1.3	17
152	Thermal radiation dominated heat transfer in nanomechanical silicon nitride drum resonators. Applied Physics Letters, 2020, 117, .	1.5	17
153	Oxide route for production of Cu2ZnSnS4 solar cells by pulsed laser deposition. Solar Energy Materials and Solar Cells, 2020, 215, 110605.	3.0	17
154	Atomic force microscope characterization of a resonating nanocantilever. Ultramicroscopy, 2003, 97, 127-133.	0.8	16
155	MEMS Bragg grating force sensor. Optics Express, 2011, 19, 19190.	1.7	16
156	Creating New VLS Silicon Nanowire Contact Geometries by Controlling Catalyst Migration. Nano Letters, 2015, 15, 6535-6541.	4.5	16
157	Fast & scalable pattern transfer via block copolymer nanolithography. RSC Advances, 2015, 5, 102619-102624.	1.7	16
158	Full-field hard x-ray microscopy with interdigitated silicon lenses. Optics Communications, 2016, 359, 460-464.	1.0	16
159	Spatial and temporal changes in the morphology of preosteoblastic cells seeded on microstructured tantalum surfaces. Journal of Biomedical Materials Research - Part A, 2009, 89A, 885-894.	2.1	15
160	Systematic study of shallow junction formation on germanium substrates. Microelectronic Engineering, 2011, 88, 347-350.	1.1	15
161	Selenium Thin-Film Solar Cells with Cadmium Sulfide as a Heterojunction Partner. ACS Applied Energy Materials, 2021, 4, 10697-10702.	2.5	15
162	Single-shot, omni-directional x-ray scattering imaging with a laboratory source and single-photon localization. Optics Letters, 2020, 45, 1021.	1.7	15

#	Article	IF	CITATIONS
163	Temperature effects in Au piezoresistors integrated in SU-8 cantilever chips. Journal of Micromechanics and Microengineering, 2006, 16, 2564-2569.	1.5	14
164	Fundamental size limitations of micro four-point probes. Microelectronic Engineering, 2009, 86, 987-990.	1.1	14
165	A MEMS Energy Harvesting Device for Vibration with Low Acceleration. Procedia Engineering, 2012, 47, 770-773.	1.2	14
166	Sensitivity of resistive and Hall measurements to local inhomogeneities: Finite-field, intensity, and area corrections. Journal of Applied Physics, 2014, 116, 133706.	1.1	14
167	Removal of low concentration contaminant species using photocatalysis: Elimination of ethene to sub-ppm levels with and without water vapor present. Chemical Engineering Journal, 2015, 262, 648-657.	6.6	14
168	Indirect tip fabrication for Scanning Probe Microscopy. Microelectronic Engineering, 1996, 30, 579-582.	1.1	13
169	FISH & amp; CHIPS: Four Electrode Conductivity / Salinity Sensor on a Silicon Multi-Sensor Chip for Fisheries Research. , 0, , .		13
170	Rate enhancement in microfabricated chemical reactors under fast forced temperature oscillations. Catalysis Communications, 2006, 7, 272-275.	1.6	13
171	Broadband light-extraction enhanced by arrays of whispering gallery resonators. Applied Physics Letters, 2012, 101, .	1.5	13
172	Self-sustained carbon monoxide oxidation oscillations on size-selected platinum nanoparticles at atmospheric pressure. Physical Chemistry Chemical Physics, 2013, 15, 2698.	1.3	13
173	Revealing origin of quasi-one dimensional current transport in defect rich two dimensional materials. Applied Physics Letters, 2014, 105, .	1.5	13
174	CMUT Electrode Resistance Design: Modeling and Experimental Verification by a Row-Column Array. IEEE Transactions on Ultrasonics, Ferroelectrics, and Frequency Control, 2019, 66, 1110-1118.	1.7	13
175	TaS <sub>2</sub> Back Contact Improving Oxide-Converted Cu <sub>2</sub> BaSnS <sub>4</sub> Solar Cells. ACS Applied Energy Materials, 2020, 3, 1190-1198.	2.5	13
176	On the Enhanced Phosphorus Doping of Nanotextured Black Silicon. IEEE Journal of Photovoltaics, 2021, 11, 298-305.	1.5	13
177	Ultralarge area MOS tunnel devices for electron emission. Physical Review B, 2007, 76, .	1.1	12
178	Microgrippers: a case study for batch-compatible integration of MEMS with nanostructures. Nanotechnology, 2007, 18, 375501.	1.3	12
179	Correlation of Effective Dispersive and Polar Surface Energies in Heterogeneous Self-Assembled Monolayer Coatings. Langmuir, 2009, 25, 5437-5441.	1.6	12
180	High quantum efficiency annular backside silicon photodiodes for reflectance pulse oximetry in wearable wireless body sensors. Journal of Micromechanics and Microengineering, 2010, 20, 075020.	1.5	12

#	Article	IF	CITATIONS
181	Sensitivity of resistive and Hall measurements to local inhomogeneities. Journal of Applied Physics, 2013, 114, .	1.1	12
182	Formation of copper tin sulfide films by pulsed laser deposition at 248 and 355Ânm. Applied Physics A: Materials Science and Processing, 2016, 122, 1.	1.1	12
183	Thermal stability of highly Sb-doped molecular beam epitaxy silicon grown at low temperatures: Structural and electrical characterization. Journal of Vacuum Science & Technology an Official Journal of the American Vacuum Society B, Microelectronics Processing and Phenomena, 1994, 12, 3016.	1.6	11
184	Cold-walled UHV/CVD batch reactor for the growth of Si1â^'xGex layers. Thin Solid Films, 1997, 294, 72-75.	0.8	11
185	Noise and sensitivity in polysilicon piezoresistive cantilevers. Chinese Physics B, 2001, 10, 918-923.	1.3	11
186	Magnetic flux generator for balanced membrane loudspeaker. Sensors and Actuators A: Physical, 2002, 97-98, 61-67.	2.0	11
187	Fabrication and modeling of narrow capillaries for vacuum system gas inlets. Journal of Applied Physics, 2005, 97, 044906.	1.1	11
188	Forced thermal cycling of catalytic reactions: Experiments and modelling. Catalysis Communications, 2007, 8, 1985-1990.	1.6	11
189	High precision micro-scale Hall effect characterization method using in-line micro four-point probes. , 2008, , .		11
190	Fusion bonding of silicon nitride surfaces. Journal of Micromechanics and Microengineering, 2011, 21, 125015.	1.5	11
191	On the pathway of photoexcited electrons: probing photon-to-electron and photon-to-phonon conversions in silicon by ATR-IR. Physical Chemistry Chemical Physics, 2012, 14, 10882.	1.3	11
192	Sacrificial structures for deep reactive ion etching of high-aspect ratio kinoform silicon x-ray lenses. Journal of Vacuum Science and Technology B:Nanotechnology and Microelectronics, 2015, 33, 062001.	0.6	11
193	Photoluminescence Imaging Induced by Laser Line Scan: Study for Outdoor Field Inspections. , 2018, , .		11
194	Black Silicon With Ultra‣ow Surface Recombination Velocity Fabricated by Inductively Coupled Power Plasma. Physica Status Solidi - Rapid Research Letters, 2019, 13, 1800477.	1.2	11
195	Wireless Photoelectrochemical Water Splitting Using Triple-Junction Solar Cell Protected by TiO2. Cell Reports Physical Science, 2020, 1, 100261.	2.8	11
196	Terahertz radiation from deltaâ€doped GaAs. Applied Physics Letters, 1994, 65, 79-81.	1.5	10
197	A compact system for large-area thermal nanoimprint lithography using smart stamps. Journal of Micromechanics and Microengineering, 2008, 18, 055018.	1.5	10
198	Investigation of Cu2ZnSnS4 nanoparticles for thin-film solar cellÂapplications. Thin Solid Films, 2017, 628, 163-169.	0.8	10

#	Article	IF	CITATIONS
199	Breakthrough in current-in-plane tunneling measurement precision by application of multi-variable fitting algorithm. Review of Scientific Instruments, 2017, 88, 095005.	0.6	10
200	Evaluation of the capacitive behavior of 3D carbon electrodes for sub-retinal photovoltaic prosthesis. Micro and Nano Engineering, 2019, 2, 110-116.	1.4	10
201	Virtual subpixel approach for single-mask phase-contrast imaging using Timepix3. Journal of Instrumentation, 2019, 14, C01011-C01011.	0.5	10
202	Anomalous activation of shallow B+ implants in Ge. Materials Letters, 2011, 65, 3540-3543.	1.3	9
203	Evaporation of Water Droplets on "Lock-and-Key―Structures with Nanoscale Features. Langmuir, 2012, 28, 9201-9205.	1.6	9
204	Sensitivity analysis explains quasi-one-dimensional current transport in two-dimensional materials. Physical Review B, 2014, 90, .	1.1	9
205	Three-dimensional nanometrology of microstructures by replica molding and large-range atomic force microscopy. Microelectronic Engineering, 2015, 141, 6-11.	1.1	9
206	Fabrication of Ni stamp with high aspect ratio, two-leveled, cylindrical microstructures using dry etching and electroplating. Journal of Micromechanics and Microengineering, 2015, 25, 055021.	1.5	9
207	Gold Nanoparticle-Based Sensors Activated by External Radio Frequency Fields. Small, 2015, 11, 248-256.	5.2	9
208	Mesoscopic current transport in two-dimensional materials with grain boundaries: Four-point probe resistance and Hall effect. Journal of Applied Physics, 2016, 120, .	1.1	9
209	H <sub>2</sub> /D <sub>2</sub> exchange reaction on mono-disperse Pt clusters: enhanced activity from minute O <sub>2</sub> concentrations. Catalysis Science and Technology, 2016, 6, 6893-6900.	2.1	9
210	Deep reactive ion etching of â€~grass-free' widely-spaced periodic 2D arrays, using sacrificial structures. Microelectronic Engineering, 2020, 223, 111228.	1.1	9
211	Devices for fatigue testing of electroplated nickel (MEMS). , 0, , .		8
212	Fish & chips: single chip silicon mems ctdl salinity, temperature, pressure and light sensor for use in fisheries research. , 0, , .		8
213	Fast micro Hall effect measurements on small pads. Journal of Applied Physics, 2011, 110, 033707.	1.1	8
214	Void-free direct bonding of CMUT arrays with single crystalline plates and pull-in insulation. , 2013, , .		8
215	Optimizing shape uniformity and increasing structure heights of deep reactive ion etched silicon x-ray lenses. Journal of Micromechanics and Microengineering, 2015, 25, 125013.	1.5	8
216	A quick look at how photoelectrodes work. Science, 2015, 350, 1030-1031.	6.0	8

#	Article	IF	CITATIONS
217	Direct bonding of ALD Al 2 O 3 to silicon nitride thin films. Microelectronic Engineering, 2017, 176, 71-74.	1.1	8
218	Tunable MEMS VCSEL on Silicon Substrate. IEEE Journal of Selected Topics in Quantum Electronics, 2019, 25, 1-7.	1.9	8
219	Spin-coated \$\$hbox {Cu}_2hbox {ZnSnS}_{4}\$\$ solar cells: A study on the transformation from ink to film. Scientific Reports, 2020, 10, 20749.	1.6	8
220	Spatial variation of the etch rate for deep etching of silicon by reactive ion etching. Journal of Vacuum Science & Technology an Official Journal of the American Vacuum Society B, Microelectronics Processing and Phenomena, 1997, 15, 993.	1.6	7
221	Uniformity-improving dummy structures for deep reactive ion etching (DRIE) processes. , 2005, 5715, 39.		7
222	Electron emission from ultralarge area metal-oxide-semiconductor electron emitters. Journal of Vacuum Science & Technology B, 2009, 27, 562.	1.3	7
223	Junction leakage measurements with micro four-point probes. AIP Conference Proceedings, 2012, , .	0.3	7
224	A transparent Pyrex μ-reactor for combined in situ optical characterization and photocatalytic reactivity measurements. Review of Scientific Instruments, 2013, 84, 103910.	0.6	7
225	Backâ€Illuminated Siâ€Based Photoanode with Nickel Cobalt Oxide Catalytic Protection Layer. ChemElectroChem, 2016, 3, 1517-1517.	1.7	7
226	Semiconductor band alignment from first principles: A new nonequilibrium Green's function method applied to the CZTSe/CdS interface for photovoltaics. , 2016, , .		7
227	Widthâ€Dependent Sheet Resistance of Nanometerâ€Wide Si Fins as Measured with Micro Fourâ€Point Probe. Physica Status Solidi (A) Applications and Materials Science, 2018, 215, 1700857.	0.8	7
228	Fabrication of an all-metal atomic force microscope probe. , 0, , .		6
229	Oxidation of methane over a Rh/Al2O3 catalyst using microfabricated reactors with integrated heating. Journal of Catalysis, 2006, 241, 74-82.	3.1	6
230	Electrical characterization of InGaAs ultra-shallow junctions. Journal of Vacuum Science and Technology B:Nanotechnology and Microelectronics, 2010, 28, C1C41-C1C47.	0.6	6
231	Electroless porous silicon formation applied to fabrication of boron–silica–glass cantilevers. Journal of Micromechanics and Microengineering, 2010, 20, 015034.	1.5	6
232	Modeling and measurements of CMUTs with square anisotropic plates. , 2013, , .		6
233	Modal radiation patterns of baffled circular plates and membranes. Journal of the Acoustical Society of America, 2014, 135, 2523-2533.	0.5	6

Precision of single-engage micro Hall effect measurements. , 2014, , .

6

#	Article	IF	CITATIONS
235	Nanoporous gyroid TiO2 and SnO2 by melt infiltration of block copolymer templates. Microporous and Mesoporous Materials, 2015, 210, 161-168.	2.2	6
236	Probing the Gas-Phase Dynamics of Graphene Chemical Vapour Deposition using in-situ UV Absorption Spectroscopy. Scientific Reports, 2017, 7, 6183.	1.6	6
237	3 <i>ï‰</i> correction method for eliminating resistance measurement error due to Joule heating. Review of Scientific Instruments, 2021, 92, 094711.	0.6	6
238	Nanocantilever based mass sensor integrated with CMOS circuitry. , 0, , .		5
239	Mechanical Characterization and Design of Flexible Silicon Microstructures. Journal of Microelectromechanical Systems, 2004, 13, 452-464.	1.7	5
240	Piezoresistance in Strained Silicon and Strained Silicon Germanium. Materials Research Society Symposia Proceedings, 2006, 958, 1.	0.1	5
241	Impact of multiple sub-melt laser scans on the activation and diffusion of shallow Boron junctions. , 2008, , .		5
242	Surface enhanced Raman spectroscopy on chip. Proceedings of SPIE, 2008, , .	0.8	5
243	Subsurface excitations in a metal. Physical Review B, 2009, 80, .	1.1	5
244	Three-way flexible cantilever probes for static contact. Journal of Micromechanics and Microengineering, 2011, 21, 085003.	1.5	5
245	High mass resolution time of flight mass spectrometer for measuring products in heterogeneous catalysis in highly sensitive microreactors. Review of Scientific Instruments, 2012, 83, 075105.	0.6	5
246	Electrostatic energy harvesting device with out-of-the-plane gap closing scheme. , 2013, , .		5
247	Two-phase model of hydrogen transport to optimize nanoparticle catalyst loading for hydrogen evolution reaction. International Journal of Hydrogen Energy, 2016, 41, 7568-7581.	3.8	5
248	Optimized electrode configuration for current-in-plane characterization of magnetic tunnel junction stacks. Measurement Science and Technology, 2017, 28, 025012.	1.4	5
249	Electrical characterization of single nanometer-wide Si fins in dense arrays. Beilstein Journal of Nanotechnology, 2018, 9, 1863-1867.	1.5	5
250	Determination of the temperature coefficient of resistance from micro four-point probe measurements. Journal of Applied Physics, 2021, 129, .	1.1	5
251	Dynamic Interfacial Reaction Rates from Electrochemistry–Mass Spectrometry. Analytical Chemistry, 2021, 93, 7022-7028.	3.2	5
252	High Mass and Spatial Resolution Mass Sensor based on Resonating Nano-Cantilevers Integrated with CMOS. , 2001, , 72-75.		5

#	Article	IF	CITATIONS
253	Current regulators for I/sup 2/L circuits to be operated from low-voltage power supplies. IEEE Journal of Solid-State Circuits, 1980, 15, 796-799.	3.5	4
254	Fabrication and characterization of flexible silicon substrates with electroplated gold leads. , 0, , .		4
255	Fabrication of high aspect ratio through-wafer vias in CMOS wafers for 3-D packaging applications. , 0, , .		4
256	Deep Reactive Ion Etching for High Aspect Ratio Microelectromechanical Components. Physica Scripta, 2004, T114, 188-192.	1.2	4
257	Self-Positioning of Polymer Membranes Driven by Thermomechanically Induced Plastic Deformation. Advanced Materials, 2006, 18, 238-241.	11.1	4
258	Parametric investigation of rate enhancement during fast temperature cycling of CO oxidation in mircroreactors. Chemical Engineering Journal, 2008, 135, S237-S241.	6.6	4
259	Determination of stress build-up during nanoimprint process in triangular polymer structures. Microelectronic Engineering, 2008, 85, 838-841.	1.1	4
260	Measurement of the resonant frequency of nano-scale cantilevers by hard contact readout. Microelectronic Engineering, 2008, 85, 1390-1394.	1.1	4
261	Giant geometrically amplified piezoresistance in metal-semiconductor hybrid resistors. Journal of Applied Physics, 2008, 104, 114510.	1.1	4
262	Electron emission from MOS electron emitters with clean and cesium covered gold surface. Applied Surface Science, 2009, 255, 7657-7662.	3.1	4
263	Solving the Helmholtz equation in conformal mapped ARROW structures using homotopy perturbation method. Optics Express, 2011, 19, 1808.	1.7	4
264	Crystallographic dependence of the lateral undercut wet etch rate of Al0.5In0.5P in diluted HCl for III–V sacrificial release. Journal of Vacuum Science and Technology B:Nanotechnology and Microelectronics, 2013, 31, .	0.6	4
265	Thermal Oxidation of Structured Silicon Dioxide. ECS Journal of Solid State Science and Technology, 2014, 3, N63-N68.	0.9	4
266	Fast static field CIPT mapping of unpatterned MRAM film stacks. Measurement Science and Technology, 2015, 26, 045602.	1.4	4
267	A variable probe pitch micro-Hall effect method. Beilstein Journal of Nanotechnology, 2018, 9, 2032-2039.	1.5	4
268	Avoiding blistering in Al2O3 deposited on planar and black Si. Solar Energy Materials and Solar Cells, 2018, 187, 23-29.	3.0	4
269	Laser ablation of high-aspect-ratio hole arrays in tungsten for X-ray applications. Microelectronic Engineering, 2019, 209, 60-65.	1.1	4
270	Batch processing of CMOS compatible feedthroughs. Microelectronic Engineering, 2003, 67-68, 487-494.	1.1	3

#	Article	IF	CITATIONS
271	Low voltage, high-Q SOI MEMS varactors for RF applications. , 0, , .		3
272	Batch fabrication of through-wafer vias in CMOS wafers for 3-D packaging applications. , 0, , .		3
273	Synthesis of crystalline Ge nanoclusters in PE-CVD-deposited SiO2 films. Applied Physics A: Materials Science and Processing, 2005, 81, 1591-1593.	1.1	3
274	PtRu Colloid Nanoparticles for CO Oxidation in Microfabricated Reactors. Catalysis Letters, 2006, 109, 7-12.	1.4	3
275	Activation of ion implanted Si for backside processing by ultra-fast laser thermal annealing: Energy homogeneity and micro-scale sheet resistance. , 2009, , .		3
276	Towards hot electron mediated charge exchange in hyperthermal energy ion–surface interactions. Journal of Physics Condensed Matter, 2010, 22, 084010.	0.7	3
277	Screen printed PZT/PZT thick film bimorph MEMS cantilever device for vibration energy harvesting. , 2011, , .		3
278	Microcutting and Forming of Thin Aluminium Foils for MEMS. Journal of Manufacturing Science and Engineering, Transactions of the ASME, 2011, 133, .	1.3	3
279	All-Optical Frequency Modulated High Pressure MEMS Sensor for Remote and Distributed Sensing. Sensors, 2011, 11, 10615-10623.	2.1	3
280	Activation and thermal stability of ultra-shallow B+-implants in Ge. Journal of Applied Physics, 2012, 112, 123525.	1,1	3
281	Preliminary Performance Evaluation of MEMS-based Piezoelectric Energy Harvesters in Extended Temperature Range. Procedia Engineering, 2012, 47, 1434-1437.	1.2	3
282	Inorganic electret with enhanced charge stability for energy harvesting. , 2013, , .		3
283	Nanoimprinted DWDM laser arrays on indium phosphide substrates. Microelectronic Engineering, 2014, 123, 149-153.	1.1	3
284	Injection molded polymeric hard X-ray lenses. Optical Materials Express, 2015, 5, 2804.	1.6	3
285	Nanomechanical Infrared Spectroscopy with Vibrating Filters for Pharmaceutical Analysis. Angewandte Chemie, 2017, 129, 3959-3963.	1.6	3
286	Effective electrical resistivity in a square array of oriented square inclusions. Nanotechnology, 2021, 32, 185706.	1.3	3
287	Silicon Nanotexture Surface Area Mapping Using Ultraviolet Reflectance. IEEE Journal of Photovoltaics, 2021, 11, 1291-1298.	1.5	3
288	In situ TEM modification of individual silicon nanowires and their charge transport mechanisms. Nanotechnology, 2020, 31, 494002.	1.3	3

#	Article	IF	CITATIONS
289	Delay Line Separation of CMUT Elements. , 2020, , .		3
290	Cu2ZnSnS4 from oxide precursors grown by pulsed laser deposition for monolithic CZTS/Si tandem solar cells. Applied Physics A: Materials Science and Processing, 2022, 128, 1.	1.1	3
291	Gettering in PolySi/SiO <i><sub>x</sub></i> Passivating Contacts Enables Si-Based Tandem Solar Cells with High Thermal and Contamination Resilience. ACS Applied Materials & Interfaces, 2022, 14, 14342-14358.	4.0	3
292	High aspect ratio MEMS capacitor for high frequency impedance matching applications. , 0, , .		2
293	SOI silicon on glass for optical MEMS. , 0, , .		2
294	Passivation of Ge Nanocrystals in SiO <sub>2</sub> . Solid State Phenomena, 2005, 108-109, 33-38.	0.3	2
295	Realtime 3D Stress Measurement in Curing Epoxy Packaging. , 2007, , .		2
296	Engineering piezoresistivity using biaxially strained silicon. Applied Physics Letters, 2008, 93, 263501.	1.5	2
297	Accurate micro Hall Effect measurements on scribe line pads. , 2009, , .		2
298	Monitoring of local and global temperature non-uniformities by means of Therma-Probe and Micro Four-Point Probe metrology. , 2009, , .		2
299	Growth and properties of self-assembled monolayers on metals. Journal of Physics: Conference Series, 2009, 152, 012029.	0.3	2
300	Study of submelt laser induced junction nonuniformities using Therma-Probe. Journal of Vacuum Science and Technology B:Nanotechnology and Microelectronics, 2010, 28, C1C21-C1C26.	0.6	2
301	Intrinsic low hysteresis touch mode capacitive pressure sensor. , 2010, , .		2
302	Micro-cantilevers for non-destructive characterization of nanograss uniformity. , 2011, , .		2
303	ZnS top layer for enhancement of the crystallinity of CZTS absorber during the annealing. , 2015, , .		2
304	Characterization of positional errors and their influence on micro four-point probe measurements on a 100 nm Ru film. Measurement Science and Technology, 2015, 26, 095005.	1.4	2
305	Optically pumped 1550nm wavelength tunable MEMS VCSEL. Proceedings of SPIE, 2016, , .	0.8	2

306 Diffusion of phosphorous in black silicon. , 2018, , .

#	Article	IF	CITATIONS
307	Vibration tolerance of micro-electrodes. Journal of Micromechanics and Microengineering, 2018, 28, 095010.	1.5	2
308	Hall effect measurement for precise sheet resistance and thickness evaluation of Ruthenium thin films using non-equidistant four-point probes. AIP Advances, 2018, 8, .	0.6	2
309	Advanced Characterisation of Black Silicon Surface Topography with 3D PFIB-SEM. , 2019, , .		2
310	Assessing the role of quantum effects in two-dimensional heterophase <mml:math xmlns:mml="http://www.w3.org/1998/Math/MathML"&gt;<mml:msub><mml:mi>MoTe</mml:mi><mml:mn>2field effect transistors. Physical Review B, 2021, 104, .</mml:mn></mml:msub></mml:math 	ıl:mini> <td>ml<b>2</b>msub&gt;</td>	ml <b>2</b> msub>
311	Novel micro-reactor flow cell for investigation ofÂmodel catalysts using <i>in situ</i> grazing-incidence X-ray scattering. Journal of Synchrotron Radiation, 2016, 23, 455-463.	1.0	2
312	Silver-substituted (Ag1-xCux)2ZnSnS4 solar cells from aprotic molecular inks. Ceramics International, 2022, 48, 21483-21491.	2.3	2
313	Flexible stamp for nanoimprint lithography. , 0, , .		1
314	High-temperature compatible nickel silicide thermometer and heater for catalytic chemical microreactors. , 0, , .		1
315	Flexible SiO <sub>2</sub> cantilevers for torsional self-aligning micro scale four-point probes. Journal of Micromechanics and Microengineering, 2007, 17, 1910-1915.	1.5	1
316	Determination of packaging induced 3D stress utilizing a piezocoefficient mapping device. , 2007, , .		1
317	Design and modeling of an all-optical frequency modulated MEMS strain sensor using nanoscale Bragg gratings. , 2009, , .		1
318	Submicron organic nanofiber devices with different anode-cathode materials: A simple approach. Journal of Vacuum Science and Technology B:Nanotechnology and Microelectronics, 2010, 28, 617-622.	0.6	1
319	Hollow core MOEMS Bragg grating microphone for distributed and remote sensing. , 2011, , .		1
320	Bio-inspired co-catalysts bonded to a silicon photocathode for solar hydrogen evolution. , 2011, , .		1
321	Quantitative mapping of large area graphene conductance. , 2012, , .		1
322	Microprobe metrology for direct sheet resistance and mobility characterization. , 2012, , .		1
323	Automated Micro Hall Effect measurements. , 2014, , .		1
324	Characterization of magnetic tunnel junction test pads. Journal of Applied Physics, 2015, 118, 143901.	1.1	1

#	Article	IF	CITATIONS
325	Black silicon solar cells with black bus-bar strings. , 2016, , .		1
326	Breakthrough in Current in Plane Metrology for Monitoring Large Scale MRAM Production. , 2017, , .		1
327	Towards solar cells with black silicon texturing passivated by a-Si:H. , 2018, , .		1
328	All-black front surfaces for building-integrated photovoltaics. Japanese Journal of Applied Physics, 2018, 57, 08RH01.	0.8	1
329	Towards diamond micro four-point probes. Micro and Nano Engineering, 2019, 5, 100037.	1.4	1
330	Electrical Contact Formation in Micro Fourâ€Point Probe Measurements. Physica Status Solidi (A) Applications and Materials Science, 2020, 217, 1900579.	0.8	1
331	Apparent size effects on dopant activation in nanometer-wide Si fins. Journal of Vacuum Science and Technology B:Nanotechnology and Microelectronics, 2021, 39, 023202.	0.6	1
332	First Experimental Results on CMOS Integrated Nickel Electroplated Resonators. Physica Scripta, 2004, T114, 184-187.	1.2	1
333	Low temperature bonding of heterogeneous materials using Al2O3 as an intermediate layer. , 2018, , .		1
334	Fabrication of integrated metallic MEMS devices. Electronics Letters, 2002, 38, 1526.	0.5	0
335	Studying different effects on the collection efficiency of a dielectrophoresis based selective filter in a microchip with integrated flow cytometers. , 0, , .		0
336	Route to batch-compatible fabrication of nanotweezers by guided self-assembly. , 2007, , .		0
337	A finite element mesh tailored to full NIL process modelling: hot embossing, cool-down and stamp release. , 2007, , .		Ο
338	Batch chemical microreactors: Reversible, in situ UHV sealing of a microcavity. Microelectronic Engineering, 2009, 86, 1389-1392.	1.1	0
339	Accuracy of micro four-point probe measurements on inhomogeneous samples: A probe spacing dependence study. , 2009, , .		Ο
340	Advanced characterization of carrier profiles in germanium using micro-machined contact probes. AIP Conference Proceedings, 2012, , .	0.3	0
341	Propagation and excitation of graphene plasmon polaritons. , 2013, , .		0
342	Excitation of plasmon modes in a graphene monolayer supported on a 2D subwavelength silicon grating. , 2013, , .		0

OLE HANSEN

#	Article	IF	CITATIONS
343	Effect of B+ Flux on the Electrical Activation of Ultra-Shallow B+ Implants in Ge. ECS Transactions, 2013, 50, 543-549.	0.3	0
344	Improvement of Infrared Detectors for Tissue Oximetry using Black Silicon Nanostructures. Procedia Engineering, 2014, 87, 652-655.	1.2	0
345	In-Situ TEM Investigation of Controlled VLS Silicon Nanowire Device Formation and Characterization. Microscopy and Microanalysis, 2016, 22, 60-61.	0.2	0
346	Protected, back-illuminated silicon photocathodes or photoanodes for water splitting tandem stacks (Conference Presentation). , 2016, , .		0
347	Indoor Measurement of Angle Resolved Light Absorption by Black Silicon. , 2017, , .		0
348	Black Silicon realized by reactive ion etching (ICP) without platen power. , 2018, , .		0
349	Towards Carrier Profiling in Nanometer-wide Si Fins with Micro Four-Point Probe. , 2018, , .		0
350	Single and double side textured black silicon require different annealing conditions for optimal passivation with ALD Al <inf>2</inf> 0 <inf>3</inf> . , 2018, , .		0
351	Methods for Fabrication of Released Nickel Comb-Drive Devices on CMOS. , 2001, , 600-603.		0
352	Micro Probe Carrier Profiling of Ultra-shallow Structures in Germanium. , 2009, , .		0
353	Wavelength tunable MEMS VCSELs for OCT imaging. , 2018, , .		0
354	Bidirectional electrostatic MEMS tunable VCSELs. , 2021, , .		0

Bidirectional electrostatic MEMS tunable VCSELs., 2021, , . 354